Return current instability in laser heated plasmas

V. T. Tikhonchuk, W. Rozmus, V. Yu. Bychenkov, C. E. Capjack, and E. Epperlein

Citation: Physics of Plasmas **2**, 4169 (1995); doi: 10.1063/1.871041
View online: https://doi.org/10.1063/1.871041
View Table of Contents: http://aip.scitation.org/toc/php/2/11
Published by the American Institute of Physics

Return current instability in laser heated plasmas

V. T. Tikhonchuk[a] and W. Rozmus
Theoretical Physics Institute, Department of Physics, University of Alberta, Edmonton, Alberta T6G 2J1, Canada

V. Yu. Bychenkov
P. N. Lebedev Physics Institute, Russian Academy of Science, Moscow 117924, Russia

C. E. Capjack
Department of Electrical Engineering, University of Alberta, Edmonton, Alberta T6G 2J1, Canada

E. Epperlein[b]
Laboratory for Laser Energetics, University of Rochester, Rochester, New York 14623-1299

(Received 5 May 1995; accepted 24 July 1995)

The localized heating of an underdense plasma by a focused laser beam has been studied with a kinetic Fokker–Planck code. Simulations show an inhibition of the electron heat flux in the region where temperature gradients are maximized. A time analysis of electron distribution function demonstrates that the heat flux inhibition does not interfere with the excitation of the return current ion acoustic instability. The conditions for onset of the instability and its possible effect on plasma transport are also discussed. © *1995 American Institute of Physics.*

I. INTRODUCTION

The issue of electron heat transport is one of the important topics in inertial confinement fusion and laser-plasma interaction physics. Proper calculation of the thermal transport coefficient is also related to more fundamental issues from the kinetic theory of plasmas, in particular studies of long time and large scale plasma response to different kinds of perturbations. It is now well recognized that the classical, diffusion-like description of thermal energy transfer in plasmas is restricted to very large scales of the temperature inhomogeneity L_T, which should be at least 100 times larger than the electron mean free path, λ_{ei}.[1] However, in many cases laser energy absorption occurs on much shorter scales, which requires a nonlocal description of the electron heat transport.[2] The delocalization of the thermal transport coefficient in these studies has been achieved by introducing a convolution term for the heat flux vector by using a kernel which extends the influence of a local classical transport coefficient over several electron mean free paths. Recent approaches use a Fourier representation of the thermal transport coefficients[3] which are derived from numerical[4] and analytical[5,6] solutions to the Fokker–Planck (FP) equation.

Another possible mechanism for the reduction of the electron heat conductivity is associated with ion acoustic turbulence.[7,8] It has been shown[9,10] that the fast electrons that conduct thermal energy from a hot plasma region also carry an electric charge which has to be compensated by the return current of cold electrons from the bulk of a distribution function. This return current drives an ion acoustic wave (IAW) instability if the drift velocity, $u_e \approx q_e / n_e T_e$, is larger than the sound speed, c_s, where q_e is the electron heat flux, and n_e, T_e are the electron density and temperature, respectively. It was shown in Ref. 11 that ion acoustic turbulence can reduce the heat flux more dramatically than nonlocal effects. However, the role played by ion acoustic turbulence is not so evident, because it develops on a time scale which is much longer than the time necessary for the nonlocal effects to occur. Also it is possible that thermal transport inhibition due to nonlocal effects may reduce the thermal flux and the return current below the threshold required for an IAW instability to occur. The last point, i.e. threshold calculations of the return current instability in the regime of nonlocal electron thermal transport, is one of the primary motivations for this study.

The IAW instability in plasmas carrying heat flux has been analyzed recently by using a phenomenological model of the nonlocal heat conductivity[12] and a simplified form for the electron distribution function. It has been found that the nonlocality of the electron thermal transport coefficient can in fact provide an independent source for an IAW instability in the long wavelength regime due to density dependence of the transport coefficient. This result has been explored further in the study of a return current instability[13] in laser produced plasmas in a geometry similar to our present model, where a cylindrically symmetric laser beam propagates through a homogeneous plasma slab. Weak turbulence theory has been used in Ref. 13 to calculate the level of ion acoustic fluctuations and their role in enhancing scattering instabilities.

In this paper we report for the first time the results of a self-consistent investigation of the return current instability in the regime of nonlocal electron heat transport. Electrons in a short plasma slab are assumed to be heated by the inverse bremsstrahlung absorption of a cylindrical laser beam and the heat flux is carried across the laser axis. The electron distribution function and the threshold of the IAW instability are found from FP simulations. These show a significant inhibition of the radial electron heat flux. However, this reduction in the thermal energy transport further increases the lin-

[a]On leave from the P. N. Lebedev Physics Institute, Russian Academy of Science, Moscow 117924, Russia.
[b]Present address: Risk & Portfolio Management, Citibank Canada, 123 Front St. West, Toronto, Ontario M5J 2M3, Canada.

ear growth rate of the return current instability, which depends primarily on the local electron temperature gradient but not on the electron heat flux.

II. SIMULATIONS OF THE LASER-PLASMA HEATING

We proceed in two steps. We first consider a Gaussian laser beam propagating through a homogeneous plasma with immobile ions. The evolution of an electron distribution function in such a plasma has been numerically calculated using the electron FP code *Spark*.[4] The plasma is assumed to be underdense and thin, so that the heat flux due to inverse bremsstrahlung (IB) laser energy absorption is predominantly in the radial direction. The initial conditions and parameters of runs are relevant to typical laser-plasma interaction experiments: the plasma is assumed to be fully ionized carbon ($Z=6$) with the initial electron temperature $T_0=300$ eV, the laser vacuum wavelength $\lambda_0=353$ nm, and the laser beam full width half maximum (FWHM) = 50 μm. We have varied the maximum of laser intensity $I=10^{14}-10^{16}$ W/cm^2 and the electron plasma density $n_e/n_c=0.02-0.5$. The code has been run in a cylindrical geometry for about 10 ps until the temperature profile reaches a quasistationary state. This time is sufficiently short so that ponderomotive effects and plasma density evolution can be neglected.[13] The FP temperature profiles, $T_e(r)$, and the electron heat fluxes, $q_e(r)$, have been compared with hydrodynamic simulations that use the classical Spitzer–Härm (SH) electron heat conductivity with different values for the flux limiter.

In the second part of our study, we use the FP electron distribution function in the collisionless dispersion equation for the IAW. The imaginary part of the IAW frequency, γ, has been calculated locally at different radial locations from the dispersion relation. The factor γ depends on position because the wavelength of IAW involves short scales, $k\lambda_{De}\lesssim 1$, as compared to the electron mean free path, $\lambda_{ei}=3T_e^2/4\sqrt{2\pi}e^4 n_e Z\Lambda$, and the laser beam width. The solution to linear dispersion relation for γ and IAW frequency ω is given by

$$\frac{\gamma}{\omega}=\frac{\pi}{4\int_0^\infty F_0(v)dv}\left(\frac{\omega}{k}F_0(0)-\frac{k_r}{k}\int_0^\infty F_1(v)dv\right), \qquad (1)$$

where we have assumed that the electron distribution function $F_e(\mathbf{v})=F_0(v)+\mu F_1(v)$ has a small anisotropic part F_1. The cosine of the angle between the IAW vector $\mathbf{k}$ and the local direction of the electron heat flux is given by μ. Higher order angular harmonics of the electron distribution function have been neglected. The IAW damping rate reaches its minimum in the direction of the heat flux ($k_r=\mathbf{k}\cdot\mathbf{r}/r$) and becomes negative if

$$P\equiv\frac{k}{\omega F_0(0)}\int_0^\infty F_1(v)dv>1. \qquad (2)$$

This condition corresponds to the threshold of the IAW instability for small ion Landau damping. The last effect is neglected in this analysis. According to the analytical theory of the return current instability,[10] which assumes the Maxwellian isotropic distribution function, $F_0=F_M$, the anisotropic part of the electron distribution function,

$$F_1(v)=\frac{1}{3}\sqrt{\frac{2}{\pi}}\frac{\lambda_{ei}}{L_T}\frac{v^4}{v_{Te}^4}\left(4-\frac{v^2}{2v_{Te}^2}\right)F_M(v), \qquad (3)$$

is proportional to the local temperature gradient, $1/L_T=|d\ln T_e/dr|$. The contribution of electron-electron collisions to the anisotropic part of the electron distribution function may be accounted for by substituting the renormalized mean free path $\lambda_{ei}^*=\lambda_{ei}(Z+0.24)/(Z+4.2)$ for λ_{ei} in Eq. (3) as proposed in Ref. 14. The substitution of F_1 given by Eq. (3) and F_M into Eq. (2) results in the following expression for the threshold parameter;

$$P=1.5\,\frac{v_{Te}}{c_s}\frac{\lambda_{ei}^*}{L_T}, \qquad (4)$$

where v_{Te} is the electron thermal velocity. In the classical theory of the electron heat conductivity, the relation between the temperature gradient and the electron heat flux is given by $q_e\equiv q_{SH}=\kappa_0 T_e/L_T$, where $\kappa_0=(128/3\pi)n_e v_{Te}\lambda_{ei}^*$. This relation allows us to rewrite Eq. (4) as

$$P=\frac{9\pi}{256}\frac{q_e}{n_e T_e c_s}. \qquad (5)$$

Equations (4) and (5) predict the threshold for the IAW instability at $\lambda_{ei}^*/L_T\gtrsim 0.11$ when the electron heat flux is about 15% of the free streaming limit. However, these are essentially the same conditions for nonlocality to occur in electron thermal transport.[4] The effects of thermal flux inhibition on the IAW instability threshold will be investigated below. We address this problem by using FP simulations of IB plasma heating by a Gaussian-shaped laser beam. The duration of the laser pulse is sufficiently short so that the plasma density does not change during the interaction time $\approx$ 10 ps. The resulting electron temperature distributions are shown in Fig. 1. Panels (a) and (b) correspond to two sets of parameters: $I=10^{15}$ W/cm^2, $n_e/n_c=0.1$ (case I) and $I=10^{16}$ W/cm^2, $n_e/n_c=0.02$ (case II) with approximately the same IB energy deposition, but different ratios of the temperature scale length to the electron mean free path. The first example corresponds to the intermediate case between classical and inhibited transport regimes, where the minimum temperature scale length, $L_T\approx 60$ μm, is 40 times larger than the electron mean free path, $\lambda_{ei}\approx 1.5$ μm. The electron heat flux shown in Fig. 2 for these parameters is inhibited by about 25% as compared to the SH value at $r=20$ μm. This results in a higher plasma core temperature and larger temperature gradient at the edge of the laser beam. The instability threshold, $P>1$, shown in Fig. 2(b) is already satisfied at distances 20–40 μm from the laser axis. Note that nonlocality and related inhibition of the heat flux, which are included in FP solutions, result in a larger value of the parameter P as compared to SH results. The maximum value of P is only 15% above the threshold at $r=30$ μm. In the case of the second example, the ratio L_T/λ_{ei} is ≈ 12 and the inhibited electron heat flux is less than 0.15 the predicted classical value. For this case the value of P is much larger than the threshold for the return current instability (cf. Fig. 3).

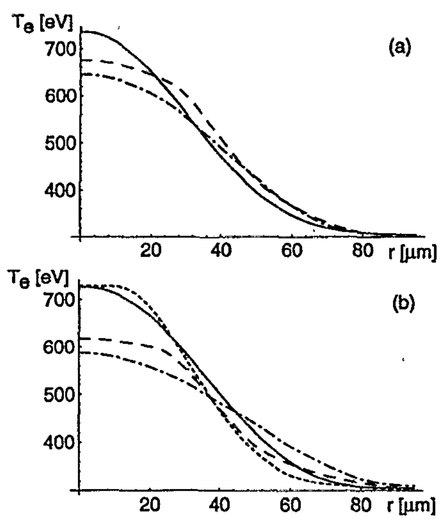

FIG. 1. Radial profiles of the electron temperature $T_e(r)$ for a carbon plasma with initial temperature $T_0=300$ eV heated by a cylindrical Gaussian laser beam with FWHM = 50 μm and wavelength $\lambda_0=353$ nm. Panel (a) is taken at time 10 ps and corresponds to the laser on-axis intensity $I=10^{15}$ W/cm^2 and plasma density $n_e/n_c=0.1$ (case I). Panel (b) is taken at time 5 ps and corresponds to the laser on-axis intensity $I=10^{16}$ W/cm^2 and plasma density $n_e/n_c=0.02$ (case II). Solid lines are the results of FP simulations, dash-dotted lines correspond to the classical SH model, dashed lines are the hydrodynamical simulations with the flux limiter f = 0.08 for the case (a) f = 0.16 for the case (b). The dotted line in panel (b) is the result of hydrodynamical simulations with the flux limiter f = 0.04 which models the effect of ion acoustic turbulence.

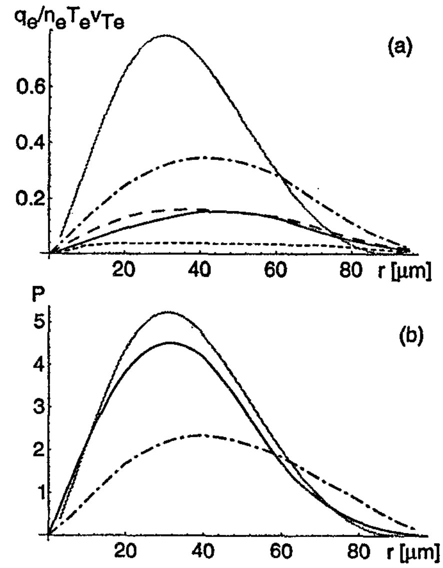

FIG. 3. Radial electron heat flux q_e (a) and IA instability parameter P (b) at time 5 ps for the parameter set of case II. Solid lines are the results of FP simulations, dash-dotted lines correspond to the classical SH model, and the dashed line is the result of hydrodynamical simulations with the flux limiter f = 0.16. Gray lines are the SH heat flux, q_{SH}, and parameter P given by Eq. (4) both evaluated from the FP temperature profile in Fig. 1(b). The dotted line in panel (a) is the result of hydrodynamical simulations with the flux limiter f = 0.04 which models the effect of ion acoustic turbulence.

III. DISCUSSION

The FP simulations clearly demonstrate that heat flux inhibition does not interfere with the return current instability. When heat flux is inhibited, Eqs. (4) and (5) are not equivalent. We have found that expression (4) is a good approximation for the parameter P if the temperature profile, $T_e(r)$, is evaluated from kinetic simulations. The radial dependence of the parameter P obtained from FP simulations and that derived from Eq. (4) is in good agreement as shown in Figs. 2(b) and 3(b). Formula (5) predicts values of P less than 1, even in the strongly driven case of Fig. 3(b). This shows that electron heat flux inhibition and the IAW instability involve different electron groups. Figure 4 illustrates this by comparing anisotropic parts of the electron distribution function from the FP model and SH theory. The instability growth rate according to Eq. (1), is related to the low

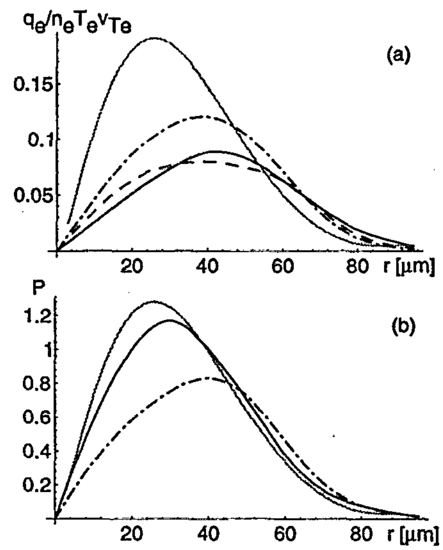

FIG. 2. Radial electron heat flux q_e (a) and IA instability parameter P (b) at time 10 ps for the parameter set of case I. Solid lines are the results of FP simulations, dash-dotted lines correspond to the classical SH model, and the dashed line is the result hydrodynamical simulations with the flux limiter f = 0.08. Gray lines are the SH heat flux, q_{SH}, and parameter P given by Eq. (4) both evaluated from the FP temperature profile in Fig. 1(a).

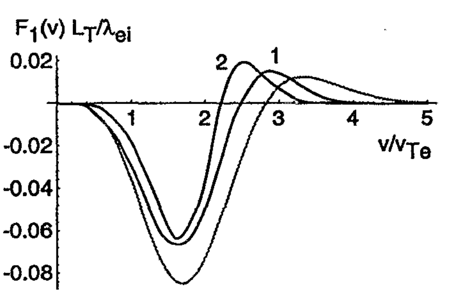

FIG. 4. Anisotropic part of electron distribution function $F_1(v)$ at $r=22.5$ μm obtained from FP simulations for case I (curve 1, time 10 ps) and case II (curve 2, time 5 ps). The gray line corresponds to the classical solution (3). Functions are normalized by $n_e\lambda_{ei}/L_Tv_{Te}^3$.

velocity moment of F_1. In addition the IAW threshold condition (4) has been derived with the assumption that electron-electron collisions do not significantly change the small velocity part of the electron distribution function, $v \lesssim v_{Te}$. Indeed, Fig. 4 shows that the FP solution does not deviate significantly from the classical SH distribution (3) for $v/v_{Te} \lesssim 2$. Contrary to the small differences found at low velocities, Fig. 4 shows a large deviation of FP solution from F_1 which is obtained using Eq. (3) for $v/v_{Te} > 2$. These differences are responsible for the strong heat flux inhibition, which is related to the higher moment of F_1: $q_e/n_eT_ev_{Te} = (2\pi/3)\int_0^\infty F_1 v^5 dv$. We have also noticed that the change in a symmetrical part of electron distribution function decreases the IAW instability threshold. According to Eq. (1), the electron Landau damping of an IAW is proportional to $F_0(0)$. For fast IB heating when $ZI/n_cT_ec > 1$, electron-electron collisions cannot equilibrate the distribution function which lacks both slow and fast electrons. This phenomenon is known as the Langdon effect.[15] For the conditions of case II, $F_0(0)$ is decreased by a factor of 2 compared with a Maxwellian distribution function.

The electron heat flux and the electron temperature obtained with FP calculations are compared with that obtained with hydrodynamical modeling in Figs. 1–3. The standard hydrodynamic equations have been solved in a cylindrical geometry with an IB heating source. The absorption coefficient includes the Langdon correction factor.[15] Due to the short heating time, the plasma density is found to remain unchanged. Energy transport has been described by using the classical SH model with a flux limiter f as a free parameter: $q_e = \min\{q_{SH}, f n_e v_{Te} T_e\}$. The approximate value of f was deduced from the FP heat flux data: f was identified as the maximum of the normalized electron heat flux from Figs. 2(a) and 3(a). An analysis of Fig. 1 demonstrates that this choice of f gives a reasonably good agreement between the kinetic and hydrodynamic results. The hydrodynamical simulations have also reproduced the correct threshold condition (4). Based on our results we can conclude that the flux-limiter approach may be a good tool for the numerical description of the underdense plasma heating. Although we did not find a simple relation between the flux-limiter value and expressions for the nonlocal electron heat flux conductivity found in different studies,[4–6] we do believe that implementation of nonlocal thermal conductivity into the hydrodynamic code may further improve the agreement with FP simulations. This has been demonstrated recently in Ref. 16 for the case of shock wave propagation.

We have shown that IB heating can produce an unstable distribution function and therefore IAW may have a significant effect on energy absorption and transport. Unlike nonlocal heat flux inhibition which occurs on the time scale of few electron-electron collision times, the time required for the IAW instability to reach the nonlinear state is a few inverse growth rates $\sim \omega_{pe}/\omega_{pi}^2(P-1)$. For the examples shown in Figs. 2 and 3 this time is approximately 5–10 ps. In the nonlinear stage, the scattering of electrons from IAW fluctuations will result in additional turbulent laser energy absorption.[8,17] The turbulence will also lead to a more isotropic electron distribution which in turn will further decrease the electron heat flux. The contribution of the IAW instability to heat flux inhibition is proportional to the parameter, $P-1$. This may be significant for our second example in Fig. 3. For that case we can apply the quasilinear theory of IAW turbulence[8,18] which predicts the inhibition of the electron heat flux for marginary stable fluctuations, $q_e \sim n_eT_ec_s$. More accurately, the theory[8,19] predicts the flux limiter factor, f_{IA},

$$q_e = f_{IA} n_e T_e v_{Te}, \quad f_{IA} = 7.5\beta\sqrt{Zm_e/m_i} \tag{6}$$

where the value of β depends on the shape of the electron distribution function F_0 and on the ratio of the plasma temperature scale length to the laser intensity scale length α. In our simulations α is always around 1. If F_0 is the Maxwellian distribution function, then $\beta = 1$. The value of β decreases to 0.26[19] for the flat-topped distribution, $F_0 \propto \exp(-\text{const}\, v^5)$. In case II, the laser intensity is sufficiently large so as to produce a significant deviation from the Maxwellian distribution. The parameter $Zv_{osc}^2/v_{Te}^2 = 2ZI/n_cT_ec$ (ratio of the IB heating time to the electron-electron collision time) equals 5.5, and this corresponds to $\beta \approx 0.32$. Therefore Eq. (6) predicts the saturation of the electron heat flux at the level equal to 0.04 of the free streaming limit. This is approximately four times smaller than the flux limiting factor f which has been used in our hydrodynamical modeling of the nonlocal heat flux inhibition. In order to predict the effect of IAW turbulence on plasma heating, the hydrodynamic modeling of case II has been made with a stronger flux limiter $f = 0.04$. As one can see in Figs. 1(b) and 3(a) (dotted lines), stronger heat flux inhibition limits the electron heat flux to a lower level and therefore further enhances the core temperature. It also produces a steeper temperature gradient because the temperature profile more closely approaches the laser intensity profile.

In conclusion, by using FP and hydrodynamical simulations of the IB laser heating of an underdense plasma, we have shown that the return current instability can be excited in the regime of electron heat flux inhibition. Its growth rate is sufficiently large to produce IAW turbulence on a 10 ps time scale and thus will further affect IB absorption and the resulting heat flux. Electron heat flux inhibition due to IAW turbulence may be comparable or even larger than that due to nonlocal effects.

ACKNOWLEDGMENTS

This work was partly supported by the Natural Sciences and Engineering Research Council of Canada and by the Russian Foundation for the Fundamental Investigations (Grant No. 93-02-15302).

[1] J. F. Luciani, P. Mora, and J. Virmont, Phys. Rev. Lett. **51**, 1664 (1983).
[2] J. R. Albritton, E. A. Williams, I. B. Bernstein, and K. P. Swartz, Phys. Rev. Lett. **57**, 1887 (1986).
[3] G. W. Hammett and F. W. Perkins, Phys. Rev. Lett. **64**, 3019 (1990); G. W. Hammett, W. Dorland, and F. W. Perkins, Phys. Fluids B **4**, 2052 (1992).
[4] E. M. Epperlein, Phys. Rev. Lett. **65**, 2145 (1990); E. M. Epperlein and R. W. Short, Phys. Fluids B **3**, 3092 (1991).
[5] A. V. Maximov and V. P. Silin, Phys. Lett. A **173**, 83 (1993); A. V. Maximov and V. P. Silin, JETP **78**, 669 (1994).
[6] V. Yu. Bychenkov, J. Myatt, W. Rozmus, and V. T. Tikhonchuk, Phys. Rev. E **50**, 5134 (1994).

[7]R. I. Bickerton, Nucl. Fusion **13**, 457 (1973); W. M. Manheimer, D. S. Colombant, and B. H. Ripin, Phys. Rev. Lett. **38**, 1135 (1977).
[8]V. Yu. Bychenkov, V. P. Silin, and S. A. Uryupin, Phys. Rep. **164**, 119 (1988).
[9]D. W. Forslund, J. Geophys. Res. **75**, 17 (1970).
[10]P. Monchicourt and P. A. Holstein, Phys. Fluids **23**, 1475 (1980).
[11]A. V. Maximov and V. P. Silin, JETP Lett. **58**, 271 (1993).
[12]V. Yu. Bychenkov, J. Myatt, W. Rozmus, and V. T. Tikhonchuk, Phys. Plasmas **1**, 2419 (1994).
[13]W. Rozmus, V. T. Tikhonchuk, V. Yu. Bychenkov, and C. E. Capjack, Phys. Rev. E **50**, 4005, (1994).
[14]E. M. Epperlein, Phys. Plasmas **1**, 109 (1994).
[15]A. B. Langdon, Phys. Rev. Lett. **44**, 575 (1980).
[16]F. Vidal, J. P. Matte, M. Casanova, and O. Larroche, Phys. Plasmas **2**, 1412 (1995).
[17]R. J. Faehl and W. L. Kruer, Phys. Fluids **20**, 55 (1977).
[18]A. A. Galeev and R. Z. Sagdeev, in *Handbook of Plasma Physics*, edited by A. A. Galeev and R. N. Sudan (North-Holland, Amsterdam, 1984), Vol. 2, p. 271.
[19]A. V. Brantov and V. Yu. Bychenkov, "Anomalous thermal transport in a plasma induced by the inverse bremsstrahlung absorption of laser radiation," Fiz. Plazmy (in press) (in Russian).